NJC

Accepted Manuscript

This is an *Accepted Manuscript*, which has been through the Royal Society of Chemistry peer review process and has been accepted for publication.

Accepted Manuscripts are published online shortly after acceptance, before technical editing, formatting and proof reading. Using this free service, authors can make their results available to the community, in citable form, before we publish the edited article. We will replace this *Accepted Manuscript* with the edited and formatted *Advance Article* as soon as it is available.

You can find more information about *Accepted Manuscripts* in the Information for Authors.

Please note that technical editing may introduce minor changes to the text and/or graphics, which may alter content. The journal's standard Terms & Conditions and the Ethical guidelines still apply. In no event shall the Royal Society of Chemistry be held responsible for any errors or omissions in this *Accepted Manuscript* or any consequences arising from the use of any information it contains.

ROYAL SOCIETY OF CHEMISTRY

www.rsc.org/njc

Journal Name

ARTICLE

$PB@Co_3O_4$ nanoparticles as both oxidase and peroxidase mimics and their application for colorimetric detection of glutathione

Received 00th January 20xx,
Accepted 00th January 20xx

DOI: 10.1039/x0xx00000x

www.rsc.org/

Wenshu Yang,[a,b] Jinhui Hao,[a,b] Zhe Zhang,[a] and Bailin Zhang*[a]

The Co_3O_4 modified Prussian blue (PB) nanocubes ($PB@Co_3O_4$) was prepared by a simple water-bath method with $CoCl_2$ as the Co source. TEM, SEM, XRD and XPS results indicate that island-like spinel phase Co_3O_4 nanoparticles (NPs) are uniformly distributed on the surface of PB nanocubes (~200 nm). The $PB@Co_3O_4$ NPs exhibit both intrinsic oxidase- and peroxidase-like activities and can quickly oxidize the peroxidase substrate 3,3',5,5'-tetramethylbenzidine (TMB) without or with hydrogen peroxide at acidic pH values. In contrast, PB nanocubes or Co_3O_4 NPs alone could not efficiently oxidize TMB without H_2O_2. The enzyme-like activity of $PB@Co_3O_4$ NPs is also influenced by the working pH and temperature. Based on the oxidase-like property of $PB@Co_3O_4$ NPs, a facile colorimetric biosensor for glutathione detection was successfully fabricated with linearity of 0.1 to 10 μM (R=0.9740) and limit of detection of 0.021 μM (S/N=3). These results demonstrate the potential applications of $PB@Co_3O_4$ NPs in bioanalysis and biodetection.

1. Introduction

Natural enzymes are a class of efficient biological catalysts involving in almost all reactions *in vivo* and have been widely applied in many fields such as biosensing, pharmaceutical processes and the food industry. However, they suffer from the high cost of preparation, purification and storage [1]. Therefore, lots of efforts are devoted to explore reliable, simple, and low-cost artificial enzyme as substitute for practical applications [2, 3]. In recent years, nanomaterials have received numerous interests due to their unique size, shape, composition, and structure-dependent properties [4, 5]. Since Fe_3O_4 nanoparticles (NPs) were found to possess the intrinsic peroxidase-like activity, lots of inorganic nanomaterials such as transition metallic NPs [6, 7], noble metal NPs [8, 9] and carbon nanomaterials [10, 11] were also exploited as enzyme mimics and have demonstrated great promises for various biodetections and biomedical applications [12, 13]. In comparison with natural enzymes, nanomaterial based enzyme mimics exhibit a high stability against harsh reaction conditions. Moreover, they possess the advantages of controlled preparation at low cost, flexibility in structure design and composition, and tunable catalytic activities.

Prussian blue (PB, $Fe_4[Fe(CN)_6]_3$), an important and interesting transition metal compound which have been reported to act as highly active peroxidase mimetics for bioassay [7, 14], can provide the ferrous ions contributing to the catalytic reaction, and has attracted much interest of many researchers [14-16]. In addition, Co_3O_4 NPs, as a kind of transition metal oxide, exhibits greater catalytic activity toward horseradish peroxidase (HRP) substrates (such as 3,3',5,5'-Tetramethylbenzidine (TMB)) compared with natural HRP [17], and other common nanocatalysts [18, 19]. Among countless examples of nanomaterials based enzyme mimics, hybrid nanomaterials are particularly impressive due to their multifunctional properties and great opportunities for catalysis [20, 21]. Very recently, many inorganic hybrid nanomaterials have been reported and realized the combination of the respective properties of each component or achieved cooperatively enhanced performances [21 22]. The combination of Co_3O_4 and PB is attractive to construct an efficient metal oxide based nanocomposites enzyme mimic.

Enlightened by the above facts, we have proposed a simple water bath method to synthesize the Co_3O_4 NPs modified PB nanocubes ($PB@Co_3O_4$ NPs) and hope to improve the catalytic properties. The as-obtained $PB@Co_3O_4$ NPs were found exhibiting both intrinsic oxidase-like and peroxidase-like activities in acidic solution. Using $PB@Co_3O_4$ NPs as oxidase mimics, a facile colorimetric method was developed for the detection of glutathione (GSH). The sensitive detection of GSH is possible by the naked eye or monitoring by a UV-Vis spectrometer. Furthermore, the proposed method does not require any nature enzyme, making it low-cost.

2. Experimental

2.1. Materials and apparatus

Poly (*N*-vinyl-2-pyrrolidone) (PVP, relative molecular mass 30,000–40,000) was obtained from Shanghai Chemical Factory (Shanghai, China). 3,3',5,5'-Tetramethylbenzidine (TMB) and

[a] Address here. State Key Laboratory of Electroanalytical Chemistry, Changchun Institute of Applied Chemistry, Chinese Academy of Sciences, Changchun 130022, (P. R. China)
E-mail: blzhang@ciac.ac.cn; Fax: +86 431-85262430; Tel: +86 431-85262430
[b] University of Chinese Academy of Sciences, Beijing 100049 (P.R. China)

glutathione (GSH) were obtained from Aladdin (Shanghai, China). H_2O_2, $K_3[Fe(CN)_6]\cdot 3H_2O$, $CoCl_2\cdot 6H_2O$ and urea were purchased from Beijing Chemical Reagent Factory (Beijing, China). Fetal bovine serum was obtained from Beijing Dingguo Biotech. Co. Ltd. Other reagents were of analytical grade and were used as received. All aqueous solutions were prepared with Milli-Q water (≥18.2 MΩ·cm) from a Milli-Q Plus system (Millipore).

UV–Vis detection was carried out on a Cary 500 UV–Vis–NIR spectrophotometer (Varian, USA). X-ray photoelectron spectroscopy (XPS) measurements were performed on an ESCALAB MKII spectrometer (VG Co., United Kingdom) with Al Kα X-ray radiation as X-ray source for excitation. Samples for XPS characterization were powders. X-ray diffraction (XRD) spectra were obtained using a D8 ADVANCE diffractometer (Bruker, Germany) using Cu Kα (0.15406 nm) radiation. Fourier transform infrared spectra (FTIR) were collected on a VERTEX 70 spectrometer (Bruker, Germany) over a range from 400 to 4000 cm^{-1}. Field emission scanning electron microscopy (FESEM) images were inspected on a Hitachi S-4800 microscopy. Energy dispersive X-ray (EDX) spectrometry was performed with a spectroscope attached to FESEM, which was used for elemental analysis. Transmission electron microscopy (TEM) and high-resolution transmission electron microscopy (HRTEM) images were obtained with a TECNAI G2 HRTEM system (Holland) under an accelerating voltage of 200 kV and a Hitachi Model H600 electron microscopy (Japan) under an accelerating voltage of 100 kV. Samples for FESEM and TEM characterizations were prepared by placing a drop of prepared solution on a silicon wafer and a carbon-coated copper grid, respectively, then dried at room temperature.

2.2. Synthesis of PB@Co_3O_4 NPs

Firstly, PB nanocubes were prepared by a simple method according to the literature [22]. In a typical procedure, PVP (3.00 g) and $K_3Fe(CN)_6\cdot 3H_2O$ (0.132 g) were added to a HCl solution (0.1 M, 40 mL) under magnetic stirring for 30 min, then the mixture was heated at 80 °C for 20 h. The obtained blue product was washed several times with deionized water and finally dried at room temperature for further use. Secondly, the as-obtained PB nanocubes (0.4 mg) were diluted in 20 mL Milli-Q water under ultrasounication for 10 minutes. Then, 6 μmol $CoCl_2\cdot 6H_2O$ and 0.36 mmol urea were added and ultrasonicated for 1 min to form a homogeneous solution. The resulting mixture was sealed and maintained at 80 °C for 24 hours. After cooled to room temperature, the product PB@Co_3O_4 was collected and washed with ethanol several times, and dried at 60 °C for 12 hours.

2.3. Detection of GSH

After reaction of 20 μg mL^{-1} PB@Co_3O_4 NPs in 2 mL 0.1M NaAc-HAc buffer (pH 3.0) and 0.5 mM TMB for 10 min at 60 °C, GSH were added to the solution keeping at 35 °C in a water bath for 10 min, then the concentration of GSH was detected by UV-Vis absorbance spectroscopy at the wavelength of 652 nm. For the real sample analysis, the fetal bovine serum was diluted 1000 times.

3. Results and discussion

3.1. Characterization of PB@Co_3O_4 NPs

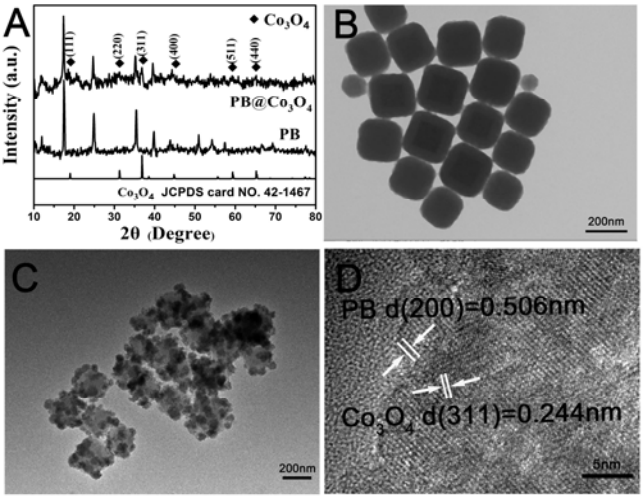

Fig. 1 XRD pattern of PB nanocubes and PB@Co_3O_4 NPs (A),TEM images of PB nanocubes (B) and PB@Co_3O_4 NPs (C), HRTEM image of PB@Co_3O_4 NPs (D).

To obtain PB@Co_3O_4 NPs, a simple water bath reaction was conducted using PB and Co^{2+} as precursors. The phase structure and relative crystallinity of as-prepared samples were firstly investigated by XRD measurement. The main diffraction peaks for PB nanocubes in the 2θ range from 10° to 80° can be easily assigned to $Fe_4[Fe(CN)_6]_3$ (JCPDS 73-687) as shown in Fig. 1A. After reacting with Co^{2+} under weak alkaline condition, PB@Co_3O_4 NPs were obtained. The characteristic peaks of PB@Co_3O_4 NPs is consistent with that of the pure PB, whereas the peak intensity decreases. The consistent peak position without shift shows that the formation of Co_3O_4 on PB nanocube surface does not dramatically affect the structure of PB nanocubes, while the intensity decrease can be explained by the formation of Co_3O_4 NPs on the nanocube surface. The characteristic peaks of Co_3O_4 marked in the XRD pattern (Fig. 1A) are well-matched with the spinel phase of Co_3O_4 (JCPDS 42-1467). These results demonstrate that there exist two phases in the reaction products, including PB and Co_3O_4.

FTIR spectra were also measured to characterize the PB and PB@Co_3O_4 NPs (Fig. S1). The FTIR spectra of PB and PB@Co_3O_4 NPs are similar to each other (Fig. S1) except that the strength of transmittance peaks belonging to H_2O (~ 3400 cm^{-1} and ~1632 cm^{-1}) increased. The strongest peak at 2083 cm^{-1} is attributed to the C≡N stretching of PB [23, 24]. The absorption located at 604 and 502 cm^{-1} can be assigned to the in-plane and out-of-plane deformations of the Fe-C bond, respectively. The stretching and in-plane deformations of the O-H appear at 1632 and 3400 cm^{-1}, respectively. The O-H bonds belong to the crystal water in PB. The similarity of these two spectra indicates that PB maintains the original crystal phase during PB@Co_3O_4 NPs formation process.

The morphology of samples was examined using the TEM (Fig. 1). The average size of as-prepared PB nanocubes with a smooth surface estimated from the TEM image are about 200 nm (Fig. 1B). When the PB nanocubes converted into

$PB@Co_3O_4$ NPs, it is found that the obtained product obviously exhibits two typical structures, including PB nanocubes and Co_3O_4 NPs, as shown in Fig.1C. High-resolution TEM image as shown in Fig. 1D, reveals that the lattice plane distance is 0.244 nm corresponding to a lattice plane distance of Co_3O_4 (311). Moreover, there is another interplanar spacing of about 0.506 nm, which can be attributed to the (200) plane of PB. This also confirms the coexistence of two kind of structures in $PB@Co_3O_4$ NPs. FESEM images of $PB@Co_3O_4$ NPs (Fig. 2A and 2B) show that the island-like Co_3O_4 NPs are uniformly distributed on the surface of PB nanocubes.

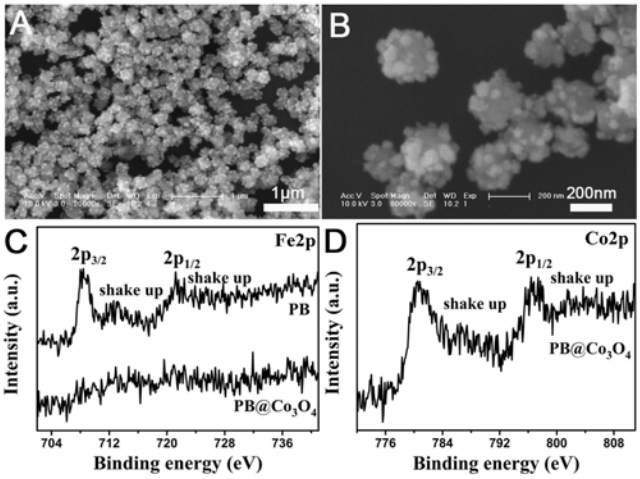

Fig. 2 FESEM images of $PB@Co_3O_4$ NPs at low (A) and high (B) magnifications. XPS spectra of Fe2p for the PB nanocubes and $PB@Co_3O_4$ NPs (C), Co2p for the $PB@Co_3O_4$ NPs (D).

The detailed elemental composition and oxidation state of the as-obtained samples were further characterized by XPS. Wide range XPS spectra of PB and $PB@Co_3O_4$ NPs as shown in Fig. S2 reveal that the later has a new Co2p peak with a relative increase of the O signal (O1s, 532 eV). The detailed Fe2p spectra (Fig. 2C) of PB and $PB@Co_3O_4$ NPs show that the binding energies of 709 eV and 722 eV are related to $Fe2p_{3/2}$ and $Fe2p_{1/2}$, respectively. When PB nanocubes converting into $PB@Co_3O_4$ NPs, the Fe2p peak decreases and the Co2p spectrum appears. We assume that the decrease intensity of Fe2p peak for $PB@Co_3O_4$ NPs is due to the modification of Co_3O_4 NPs on the surface of PB nanocubes (Fig. 2C). The peaks of 780 eV and 797 eV (Fig. 2D) were corresponding to $Co2p_{3/2}$ and $Co2p_{1/2}$, respectively, with two shakeup satellite [25]. The appearance of those two characteristic peaks and the satellites nearby further confirms the presence of Co^{2+} and Co^{3+} in Co_3O_4 NPs, which is considered the key for their catalytic properties [17].

3.2. Detection of GSH

More recently, the peroxidase-like activities of PB and Co_3O_4 NPs have been reported [7, 17]. In this study, the as-synthesized $PB@Co_3O_4$ NPs could catalyze the oxidation of peroxidase substrate (OPD and TMB) in the presence of H_2O_2, as shown in Fig.S3. Furthermore, the oxidation of OPD and TMB was easily visualized by the formation of the colored product after adding catalyst (Fig.S3 and S4), indicating that $PB@Co_3O_4$ NPs can act as oxidase mimics. These results demonstrate the $PB@Co_3O_4$ NPs exhibit both oxidase- and peroxidase-like activities. With the same concentration of catalyst under optimal pH and temperature of PB, Co_3O_4 (Fig.S5) and $PB@Co_3O_4$, respectively, control experiments showed that PB and Co_3O_4 NPs have not appreciable catalytic activity for the oxidation of substrates without H_2O_2 (Fig. 3A) and the catalytic activity of $PB@Co_3O_4$ NPs was remarkably enhanced.

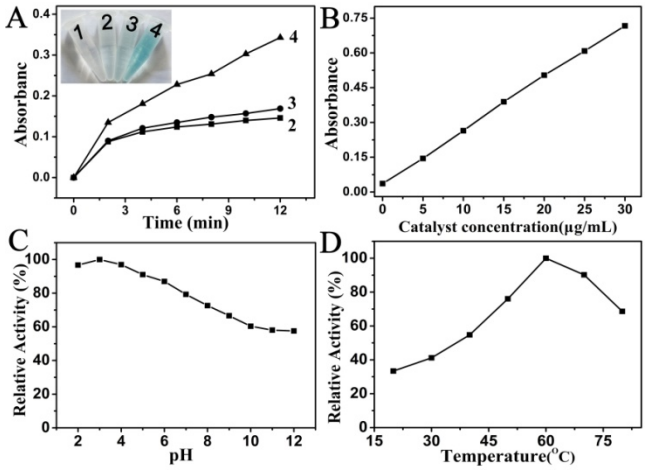

Fig.3 (A) The time-dependent absorbance changes at 652 nm of TMB reaction solutions in the presence of different catalysts: PB (2), Co_3O_4(3) and $PB@Co_3O_4$ with the same concentration under optimal pH and temperature, respectively. (Inset: Photograph of different systems: H_2O(1); PB+TMB (2); Co_3O_4+TMB (3) and $PB@Co_3O_4$+TMB (4)). Dependence of the oxidase-like activity of $PB@Co_3O_4$ NPS on catalyst concentration (B), pH (C) and temperature (D).

Subsequently, the TMB was selected as the substrate to investigate the enzyme-like activity of $PB@Co_3O_4$ NPs. The oxidase-like activity was firstly investigated at different catalyst concentration (Fig. 3B), pH (Fig. 3C) and temperature (Fig. 3D). With increase of catalyst concentration, the absorbance of TMB solution was also increased (Fig. 3B). When the pH and temperature were approximately 3.0 and 60 °C, the $PB@Co_3O_4$ NPs showed the best catalytic performance. Moreover, the peroxidase-like property of $PB@Co_3O_4$ NPs was also studied. As shown in Fig. S6, the enzymatic properties of catalyst were affected by pH, temperature, and H_2O_2 concentration, which is similar to that of HRP.

To investigate the mechanism of oxidase-like activity of $PB@Co_3O_4$, two radical inhibitors (benzoquinone and isopropyl alcohol) were used to evaluate the capability of $PB@Co_3O_4$ generating reactive oxygen species (ROS) (Fig.S7). When 0.5 mM benzoquinone, known as $O_2^{-}\cdot$ scavenger, was added to the $PB@Co_3O_4$-TMB system, the oxidase-like activity of $PB@Co_3O_4$ was suppressed. Therefore, $O_2^{-}\cdot$ plays an important role in the oxidase-like activity of $PB@Co_3O_4$. A possible mechanism was proposed on the oxidase-like activity of $PB@Co_3O_4$: according to previous reports, O_2 dissolved in water can be absorbed on the surface of $PB@Co_3O_4$ and the O-O bond might be broken up into ROS by virtue of the catalysis of $PB@Co_3O_4$. The generated ROS ($O_2^{-}\cdot$) can react with TMB to produce a blue color [26].

Furthermore, XRD (Fig.S8), SEM (Fig.S9) and EDX (Fig.S9) characterizations of PB@Co_3O_4 NPs were conducted after the oxidase-like catalytic reaction. The XRD patterns of PB@Co_3O_4 NPs indicates that it is still PB@Co_3O_4 in nature after catalytic reaction (Fig.S8) and the morphology and composition of PB@Co_3O_4 NPs have no significant change (Fig.S9). All these demonstrate that the stability of the PB@Co_3O_4 NPs is good as oxidase mimic.

GSH, which has an indispensable role in maintaining the reducing environment in cells meanwhile protecting cells against oxidative stress, is an important redox regulator in cells of plants and animals [27]. Therefore, the level of intracellular GSH has become an important indicator in monitoring the overall health of cells and their ability to protect cells against oxidative damage [21]. As it is a recognizably valuable biomarker in a variety of diseases, the detection of GSH has been becoming an interesting subject. The as-prepared PB@Co_3O_4 NPs could catalyze the fast oxidation of TMB without H_2O_2 to produce a deep blue color (maximum absorbance 652 nm) within 10 min under optimized conditions. The addition of GSH can reduce the oxidized TMB, resulting in a fading of solution color and a decrease of UV-Vis absorbance (ΔA). Based on the oxidase-like property of as-prepared PB@Co_3O_4 NPs, a novel colorimetric method for detecting GSH was established. As shown in Fig. 4, the curve of GSH detection was obtained between ΔA and the concentration of GSH under the optimal conditions. The limit of detection (LOD) for GSH was estimated as low as 0.021 μM with a linear range from 0.1 to 10 μM (R=0.9740) (Fig.4). The LOD obtained by this study was better than that of some other colorimetric methods (0.1 μM and 0.5 μM) [28, 29].

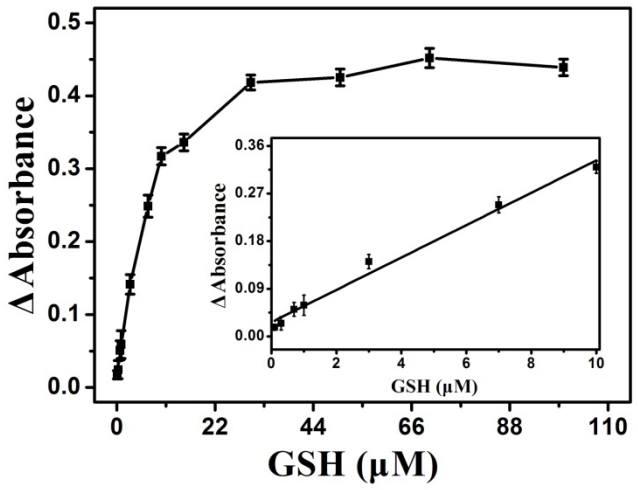

Fig. 4 The dose-response curves for UV-vis detection of GSH using PB@Co_3O_4 NPs as the oxidase mimic. Inset: The linear calibration plots for GSH determination. The error bars represent the standard deviation of the three measurements.

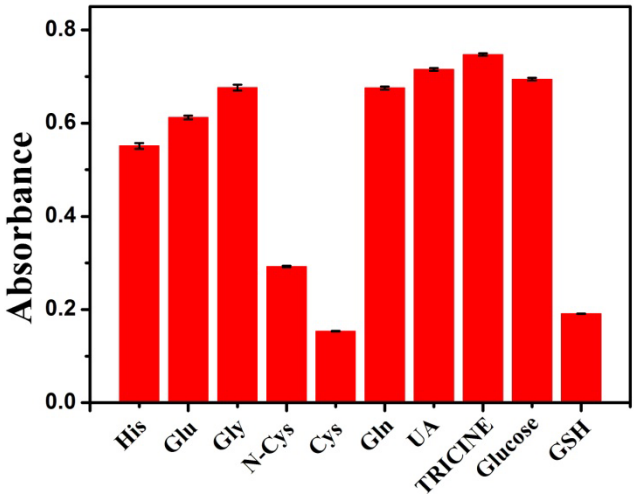

Fig. 5 UV-vis absorbance at 652 nm of PB@Co3O4 NPs and TMB solution after addition of 20 μM of L-histidine, glutamic acid, glycine, N-acetyl-L-cysteine, cysteine, glutamine, uric acid, n-[2-hydroxy-1, 1-bis (hydroxymethyl) ethyl]-glycin, glucose and GSH.

The colorimetric response to some amino acids and other substances under the similar conditions, such as *L*-histidine (His), glutamic acid (Glu), glycine (Gly), *N*-acetyl-*L*-cysteine (N-Cys), cysteine (Cys), glutamine (Gln), uric acid (UA), *n*-[2-hydroxy-1,1-bis(hydroxymethyl) ethyl]-glycin (TRICINE), and glucose was summarized in the histogram as shown in Fig. 5. The results indicated that except for Cys, *N*-Cys and GSH, the addition of all other species have not markedly decreased the absorbance intensity of TMB solution. This observation demonstrates the degree of catalytic reduction of oxidized TMB with GSH benefited from the thiol agent. The colorimetric method for GSH detection exhibits a good selectivity and can further be applied to the biological samples. On the basis of the results obtained, we further studied the possible applicability of the sensor array for the direct measurement of GSH in fetal bovine serum. The practical samples were spiked with certain amounts of GSH and the results were given in Table 1. The recoveries of the practical samples are in the range from 91.21% to 110.32%. The desirable recoveries demonstrate the reliability of the proposed method for detection of GSH in practical applications.

Table 1 Results for the determination of GSH in serum samples.

Serum sample	Glutathione spiked(μM)	Glutathione measured (μM)	Recovery (%)	RSD (n = 3)
Fetal Bovine Serum	0	3.57		1.52
	4	7.98	110.32	3.60
	5	8.28	94.14	2.52
	10	12.69	91.21	1.58

4. Conclusions

In summary, we have prepared Co_3O_4 nanoparticles modified Prussian blue naocubes through facile water bath method and found the PB@Co_3O_4 nanoparticles possess both intrinsic oxidase- and peroxidase-like activities. The combination of

Prussian blue and Co_3O_4 has remarkably enhanced the catalytic property of nanomaterials. Based on the mimic oxidase property of PB@Co_3O_4 nanoparticles, a highly sensitive colorimetric detection method for glutathione was developed. The linear range was from 0.1 to 10 μM with the detection limit of 0.021 μM. The present study shows a new possibility for the rapid, facile detection of glutathione with good sensitivity, which may be of use to the biomedical research community.

Acknowledgements

This work is supported by the National Natural Science Foundation of China(No. 21375122).

Notes and references

1 J. Xie, X. Zhang, H. Wang, H. Zheng and Y. Huang, Trac-trend. Anal. Chem., 2012, 39, 114-129.
2 A.X. Zheng, Z.X. Cong, J.R. Wang, J. Li, H.H. Yang and G.N. Chen, Biosens. Bioelectron., 2013, 49, 519-524.
3 H. Jiang, Z.H. Chen, H.Y. Cao and Y.M. Huang, Analyst, 2012, 137, 5560-5564.
4 P.C. Pandey and A.K. Pandey, Analyst, 2013, 138, 2295-2301.
5 Y. Liang, Q. Liu, A.M. Asiri, X. Sun and Y. Luo, ACS Catalysis, 2014, 4, 4065-4069.
6 P. Biparva, S.M. Abedirad and S.Y. Kazemi, Talanta, 2014, 130, 116-121.
7 W.M. Zhang, D. Ma and J.X. Du, Talanta, 2014, 120, 362-367.
8 H.Y. Chen, Y. Li, F.B. Zhang, G.L. Zhang and X.B. Fan, J. Mater. Chem., 2011, 21, 17658-17661.
9 X.X. Wang, Q. Wu, Z. Shan and Q.M. Huang, Biosens. Bioelectron., 2011, 26, 3614-3619.
10 X. Wang, K. Qu, B. Xu, J. Ren and X. Qu, Nano Research, 2011, 4, 908-920.
11 Y. Song, X. Wang, C. Zhao, K. Qu, J. Ren and X. Qu, Chem.-Eur. J., 2010, 16, 3617-3621.
12 Y. Fan and Y. Huang, Analyst, 2012, 137, 1225-1231.
13 X. Guo, Y. Wang, F. Wu, Y. Ni and S. Kokot, Analyst, 2015, 140, 1119-1126.
14 X.-Q. Zhang, S.-W. Gong, Y. Zhang, T. Yang, C.-Y. Wang and N. Gu, J. Mater. Chem., 2010, 20, 5110-5116.
15 B. Zargar and A. Hatamie, Anal Methods, 2014, 6, 5951-5956.
16 L. Gao, J. He, W. Xu, J. Zhang, J. Hui, Y. Guo, et al., Biosens. Bioelectron., 2014, 62, 79-83.
17 J.L. Dong, L.N. Song, J.J. Yin, W.W. He, Y.H. Wu, N. Gu, et al., Acs Appl. Mater. Interfaces, 2014, 6, 1959-1970.
18 X.H. Li, Z.J. Zhang and Y.B. Li, Biochem. Biotech., 2014, 172, 1859-1865.
19 X. Li, Z. Zhang, L. Tao and M. Gao, Spectrochim. Acta A, 2013, 107, 311-316.
20 Z. Zhang, J. Hao, W. Yang, B. Lu, X. Ke and B. Zhang, Acs Appl. Mater. Interfaces, 2013, 5, 3809-3815.
21 S. Bi, T. Zhao, X. Jia and P. He, Biosens. Bioelectron., 2014, 57, 110-116.
22 M. Hu, A.A. Belik, M. Imura and Y. Yamauchi, J. Am. Chem. Soc., 2012, 135, 384-391.
23 L. Shen, Z.X. Wang and L.Q. Chen, Chem. Eur. J., 2014, 20, 12559 -12562.
24 X. Q. Zhang, S. W. Gong, Y. Zhang, T. Yang, C. Y. Wang and N. Gu, J. Mater.Chem., 2010, 20, 5110– 5116.
25 X.Y. Niu, Y.Y. Xu, Y.L. Dong, L.Y. Qi, S.D. Qi and H.L. Chen, J. Alloy. Compd., 2014, 587, 74-81.
26 Y.H. Xiong, S.H. Chen, F.G. Ye, L.J. Su, C. Zhang, S.F. Shen and S.L. Zhao, Anal. Methods, 2015, 7, 1300–1306.
27 A. Pompella, A. Visvikis, A. Paolicchi, V. De Tata and A.F. Casini, Biochem. Pharmacol., 2003, 66, 1499-1503.
28 X. Liu, Q. Wang, Y. Zhang, L.C. Zhang, Y.Y. Su and Y. Lv, New J. Chem., 2013, 37, 2174-2178.
29 B. Hu, X. Cao and P. Zhang, New J. Chem., 2013, 37, 3853-3856.

Graphical Abstract

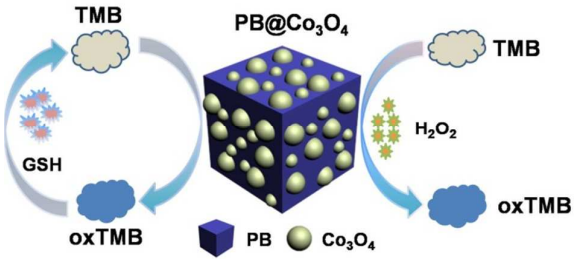

Co_3O_4 modified Prussian blue nanocubes (PB@Co_3O_4) was obtained through water-bath method and found exhibiting both intrinsic oxidase-like and peroxidase-like activities.